NUWC-NPT Reprint Report 11,907
1 March 2009

Nonlinear Acoustics in Cicada Mating Calls Enhance Sound Propagation

Derke R. Hughes
Albert H. Nuttall
Richard A. Katz
G. Clifford Carter
Sensors and Sonar Systems Department

Naval Undersea Warfare Center Division
Newport, Rhode Island

Reprint of an article from the *Journal of the Acoustical Society of America*, vol. 125, no. 2, February 2009.

Nonlinear acoustics in cicada mating calls enhance sound propagation

Derke R. Hughes,[a] Albert H. Nuttall,[b] Richard A. Katz, and G. Clifford Carter
Naval Undersea Warfare Center Division, Newport, 1176 Howell Street, Newport, Rhode Island 02841-1708

(Received 3 May 2008; revised 31 October 2008; accepted 15 November 2008)

An analysis of cicada mating calls, measured in field experiments, indicates that the very high levels of acoustic energy radiated by this relatively small insect are mainly attributed to the nonlinear characteristics of the signal. The cicada emits one of the loudest sounds in all of the insect population with a sound production system occupying a physical space typically less than 3 cc. The sounds made by tymbals are amplified by the hollow abdomen, functioning as a tuned resonator, but models of the signal based solely on linear techniques do not fully account for a sound radiation capability that is so disproportionate to the insect's size. The nonlinear behavior of the cicada signal is demonstrated by combining the mutual information and surrogate data techniques; the results obtained indicate decorrelation when the phase-randomized and non-phase-randomized data separate. The Volterra expansion technique is used to fit the nonlinearity in the insect's call. The second-order Volterra estimate provides further evidence that the cicada mating calls are dominated by nonlinear characteristics and also suggests that the medium contributes to the cicada's efficient sound propagation. Application of the same principles has the potential to improve radiated sound levels for sonar applications. [DOI: 10.1121/1.3050258]

PACS number(s): 43.60.Wy, 43.25.Ts, 43.80.Jz [EJS] Pages: 958–967

I. INTRODUCTION

A. Background

The objective of this research is to begin to understand how the cicada, a small insect, emits one of the loudest sounds in all of the insect population despite its relatively small size. Detailed knowledge of the characteristics of the cicada's acoustic signature is a necessary step toward the ultimate goal of transferring this biotechnological feat of nature to a manmade transduction system of similar proportions. The cicada's highly effective sound production system occupies a physical space typically less than 3 cc. Cicadas are sexually dimorphic, and only males possess the structures necessary for making loud audible sounds. Male sounds are broadcast advertisements for attracting females, and they are typically loud, rhythmic, and easily distinguished from background noise. Males create sound by flexing a pair of ridged abdominal membranes called tymbals. The sounds made by these tymbals are amplified by the hollow abdomen functioning as a tuned resonator, as described by current research.[1–6] Nevertheless, the tuned resonator explanation in the current literature does not account for the sound radiation capabilities of the cicada.[7]

Studying the sound production system of the cicada in captivity has some inherent difficulties: cicadas vocalize only on sunny days and do not respond as well to indoor lighting. However, the recent discovery of a female response to the mating call of the male has made it possible to conduct experiments on cicadas in the field. In many species, the females answer loud male signals with quiet wing flick responses.[8–10] Males perceiving such responses will approach that signal and continue to call even if disturbed. These female signals are easily imitated, which provides an important tool for collecting and manipulating cicadas: in an acoustical duet with a female, a male will become sexually excited and continue to sing even if disturbed or manipulated. Similar manipulations without a duet may cause a male to stop calling.

B. Current experimental opportunities with periodic cicadas

Opportunities to collect and study cicadas of the midwestern and eastern United States are limited by the insects' periodical cycles. The insects have a 13 or 17 year life cycle and emerge in mass numbers, known as broods, at predictable times in predictable locations.[11,12] Since the sounds and behaviors of the cicadas are not as yet fully characterized,[8] an upcoming emergence of the insects will provide an opportunity to test and report on the tymbal and abdomen structural dynamics that generate the cicada's mating call. Measuring the cicada's two most important anatomic structures for producing sound would add to the scientific understanding of the extent of the nonlinear nature of the cicada signals and would also help to explain the high sound levels produced by this small insect.

C. Current state of cicada research

A comprehensive review of the prominent journal articles on cicada sound production and mechanisms[13–19] and a survey of a number of subject area expert textbooks in this field[20–28] revealed that the mechanisms underlying the cicada's sound levels and efficient sound propagation are not

[a]Author to whom correspondence should be addressed. Electronic mail: derke.hughes@navy.mil
[b]Retired.

fully understood. The cicada song has been classically modeled using linear mathematical methods. However, these linear methods are insufficient for a true model of the system because the buckling tymbals within the cicada sound production system are essential to the acoustic level and propagation of this mating call. Inelastic buckling is well recognized as a nonlinear phenomenon among researchers.[29]

II. QUANTIFYING NONLINEARITY IN CICADA SIGNALS

A. Technical approach

A signal processing repertoire includes methods to test for (a) Gaussianity, (b) non-Gaussianity, (c) linearity, and (d) nonlinearity. The basic analytical tools used to perform these tests are the temporal power spectrum, the average mutual information (Mi) (i.e., an information theory technique), and surrogate data hypothesis testing (i.e., phase randomization). A preliminary determination of the degree and influence of these effects in the sound production system of the cicada is explored using the Volterra expansion.

B. Nonlinear signal processing with mutual information

In order to substantiate the existence of nonlinearity, a quantitative method must be established. This study used Mi (Ref. 30) and a surrogate data method to confirm nonlinearity. Equation (1), which defines the general Mi, is a probabilistic equation used quantitatively to assess information between two random variables A and B.

$$I_{A,B} = \sum_{i,j} P_{AB}(a_i,b_j)\log_2\left[\frac{P_{AB}(a_i,b_j)}{P_A(a_i)P_B(b_j)}\right], \tag{1}$$

where $P_{AB}(a_i,b_j)$ is the joint probability of events from sets $A=\{a_i\}$ and $B=\{b_j\}$, and $P_A(a_i)$ and $P_B(b_j)$ are the marginal individual probabilities associated with sets A and B, respectively. For example, set B can be taken as a collection of events that are time-delayed versions of the events in set A, which is the case for this research.

The surrogate data method consists of randomizing the phase of a signal spectrum as shown in

$$\begin{aligned} \mathbf{s}(n) &= \sum_{k=0}^{N-1} x(k)e^{-i2\pi nk/N} \quad \text{for } n = 0{:}N-1. \\ \mathbf{S}(k) &= \sum_{n=0}^{N/2-1} \mathbf{s}(n)e^{i[\varphi(n)+2\pi nk/N]} \\ &\quad + \sum_{n=N/2}^{N-1} \mathbf{s}(n)e^{i[-\varphi(n)+2\pi nk/N]} \quad \text{for } k = 0{:}N-1. \end{aligned} \tag{2}$$

$\mathbf{S}(k)$ is the overall phase-randomized discrete Fourier transform (DFT) of signal $\mathbf{x}(k)$, where phases $\{\varphi(n)\}$ are independent, uniform, and randomly distributed over a 2π range. $\mathbf{s}(n)$ is the complex amplitude spectrum of the DFT of the original time series, which is altered by a random phase $\varphi(n)$. In the surrogate method, the inverse DFT, $\mathbf{S}(k)$, is calculated from $\mathbf{s}(n)$, and this transformed time series is called the surrogate data and used for a comparison with the original signal $x(k)$. Nonlinearity exists if the randomized signal's Mi diverges from the original signal's Mi, thereby signifying that nonlinearity must be present in the time series.[31]

Linear calculations are plotted with the nonlinear signal results in order to display the contrast between linearity and nonlinearity. The Gaussian rule in Eq. (3) is presented to indicate how the correlation coefficient and Mi are linked for the special case of a pair of Gaussian random variables with normalized correlation coefficient ρ:[32]

$$I_{A,B} = -\tfrac{1}{2}\log_2(1-\rho^2). \tag{3}$$

Note that the Mi $I_{A,B}$ is 0 when the correlation coefficient ρ is 0, while the Mi goes to infinity as the correlation coefficient goes to positive or negative 1. This holds for all joint Gaussian processes, which are considered linear processes. The frequency domain equivalent of the correlation coefficient for measuring linearity is the subject of many published papers on coherence in the 1993 reprint text by Carter.[33] Papers on coherence include how to estimate coherence, how to minimize bias and variance, and how to determine confidence bounds for estimates of magnitude-squared coherence. In general, for stationary random process, proper averaging of large time segment improves estimation.

C. Higher-order spectral techniques using magnitude-squared bicoherence

Furthermore, multispectral techniques exist, such as bicoherence and tricoherence, which could provide additional understanding of a non-Gaussian process. If the cicada signals are non-Gaussian, the bicoherence could determine if a process is a mixed-phased process or a nonlinear process. Cumulants are higher-order statistical information about any data series. For example, the first-order cumulant for a stationary process is its mean value. The second-order cumulant for a zero-lag process is the covariance, the third is skewness, and the fourth is kurtosis. As the first step beyond first-order spectral analysis, this study analyzes the bicoherence. Equation (4) is the magnitude-squared bicoherence (MSB), which is used to provide evidence on whether a data sequence is linear or nonlinear:

$$B(f_1,f_2) = \frac{|S_2(f_1,f_2)|^2}{S(f_1)S(f_2)S(f_1+f_2)}. \tag{4}$$

D. Nonlinear signal processing using a Volterra expansion

A nonlinear fit is performed on the cicada data by means of the Volterra expansion, which describes the first-order and second-order signal dynamics present within the cicada time series. The data acquired on the cicada consist of two laser measurements, denoted by sequences $\{\mathbf{a}(n)\}$ and $\{\mathbf{b}(n)\}$, as well as a simultaneously sampled microphone sequence $\{\mathbf{z}(n)\}$. This situation will be considered to be a two-input, one-output, nonlinear "cicada system" with mathematical memory, instead of the traditional system of one input and one output.[34] This formulation lends itself to a Volterra ex-

pansion, which can be used to determine, quantitatively, the extent of nonlinearity present between the two inputs and the one output.

1. Second-order Volterra formulation

The standard Volterra expansion for a one-input system takes the form

$$\mathbf{y}(n) = \mathbf{h}_0 + \sum_{k=0}^{K_1-1} \mathbf{h}_1(k)\mathbf{a}(n-k) + \sum_{k=0}^{K_2-1}\sum_{j=k}^{K_2-1} \mathbf{h}_2(k,j)\mathbf{a}(n-k)\mathbf{a}(n-j), \quad (5)$$

when carried to the second order, where $\mathbf{y}(n)$ is the Volterrra fit. The three functions $\mathbf{h}_0, \mathbf{h}_1(k)$, and $\mathbf{h}_2(k,j)$ are the zeroth-order, first-order, and second-order kernels, respectively. The first-order terms are carried out to length K_1, while the second-order terms are carried out to length K_2 by K_2. Because of the symmetry inherent to $\mathbf{h}_2$ in Eq. (5), the summation index j can be limited to value k and above. The unknown kernels appear *linearly* in model Eq. (5), whereas the *known* excitation $\{\mathbf{a}(n)\}$ appears nonlinearly through a product of delayed versions.

With a two-input model, a generalization is necessary, namely,

$$\mathbf{y}(n) = \mathbf{y}_0 + \mathbf{y}_1(n) + \mathbf{y}_2(n), \quad (6)$$

where components

$$\mathbf{y}_1(n) = \sum_{k=0}^{K_1-1} \mathbf{h}_\mathbf{a}(k)\mathbf{a}(n-k) + \sum_{k=0}^{K_1-1} \mathbf{h}_\mathbf{b}(k)\mathbf{b}(n-k), \quad (7)$$

$$\mathbf{y}_2(n) = \sum_{k=0}^{K_2-1}\sum_{j=k}^{K_2-1} \mathbf{h}_{\mathbf{aa}}(k,j)\mathbf{a}(n-k)\mathbf{a}(n-j) + \sum_{k=0}^{K_2-1}\sum_{j=k}^{K_2-1} \mathbf{h}_{\mathbf{bb}}(k,j)\mathbf{b}(n-k)\mathbf{b}(n-j) + \sum_{k=0}^{K_2-1}\sum_{j=0}^{K_2-1} \mathbf{h}_{\mathbf{ab}}(k,j)\mathbf{a}(n-k)\mathbf{b}(n-j).$$

There are two linear components in $\{\mathbf{y}_1(n)\}$ each of length K_1, and three nonlinear (second-order) components in model output $\{\mathbf{y}_2(n)\}$. The advantage of the inherent symmetry in the two auto components in $\mathbf{y}_2(n)$ reduces the number of kernel values that have to be determined. However, the cross component $\mathbf{h}_{\mathbf{ab}}(k,j)$ in $\mathbf{y}_2(n)$ has no such symmetry and therefore requires a full K_2 by K_2 expansion. The total number of unknown kernel coefficients in Eqs. (6) and (7) is

$$K = 1 + 2K_1 + K_2(2K_2 + 1). \quad (8)$$

It is desired to choose these coefficients $\mathbf{h}$ so that the *total* model output, Eq. (6), fits the measured microphone output $\mathbf{z}(n)$ as well as possible using least squares, so that $\mathbf{y}(n) \approx \mathbf{z}(n)$. The least-squares approach is adopted because the simultaneous equations for the optimum kernel coefficients will then all be linear.

Although the laser and microphone data have been sampled at frequency f_s=96 kHz, the crucial frequency content of the cicada system itself is not believed to extend above 10 kHz. Therefore, reductions in the memory lengths K_1 and K_2 for the first-order and second-order kernels in the model will not alias the cicada statistical information. Also, the memory lengths are decreased to minimize the computer random access memory required to calculate Eq. (6). Consequently, a decimation factor of M is applied to the kernels. Thus, the model to be fitted is a modification of Eq. (7), namely,

$$\mathbf{y}_1(n) = \sum_{k=0}^{K_1-1} \mathbf{h}_\mathbf{a}(k)\mathbf{a}(n-Mk) + \sum_{k=0}^{K_1-1} \mathbf{h}_\mathbf{b}(k)\mathbf{b}(n-Mk) \equiv \mathbf{y}_\mathbf{a}(n) + \mathbf{y}_\mathbf{b}(n), \quad (9)$$

$$\mathbf{y}_2(n) = \sum_{k=0}^{K_2-1}\sum_{j=k}^{K_2-1} \mathbf{h}_{\mathbf{aa}}(k,j)\mathbf{a}(n-Mk)\mathbf{a}(n-Mj) + \sum_{k=0}^{K_2-1}\sum_{j=k}^{K_2-1} \mathbf{h}_{\mathbf{bb}}(k,j)\mathbf{b}(n-Mk)\mathbf{b}(n-Mj) + \sum_{k=0}^{K_2-1}\sum_{j=0}^{K_2-1} \mathbf{h}_{\mathbf{ab}}(k,j)\mathbf{a}(n-Mk)\mathbf{b}(n-Mj) \equiv \mathbf{y}_{\mathbf{aa}}(n) + \mathbf{y}_{\mathbf{bb}}(n) + \mathbf{y}_{\mathbf{ab}}(n).$$

By this means, the memory length of the first-order kernels is MK_1 units of the sampling increment $1/f_s$, while that of the second-order kernels is MK_2 units. Notice that the measured data $\mathbf{a}(n)$, $\mathbf{b}(n)$, and $\mathbf{z}(n)$ are *not* decimated, thereby retaining any harmonic and intermodulation products that might have been created by the cicada system itself.

2. Least-squares considerations

The details of a first-order fitting procedure will be presented; this formulation can then be extended to include all the terms in Eq. (9). The pertinent equation that governs the least-squares approach is to make

$$\mathbf{y}_\mathbf{a}(n) = \sum_{k=0}^{K_1-1} \mathbf{h}_\mathbf{a}(k)\mathbf{a}(n-Mk) = \mathbf{h}_\mathbf{a}(0)\mathbf{a}(n) + \mathbf{h}_\mathbf{a}(1)\mathbf{a}(n-M) + \cdots + \mathbf{h}_\mathbf{a}(K_1-1)\mathbf{a}(n-M(K_1-1)) \quad (10)$$

approximate $\mathbf{z}(n)$ for

$$N_1 \le n \le N_t, \quad N_1 \equiv M(K_1-1)+1, \quad (11)$$

where N_t is the common data length of the three available data sequences. The particular starting value N_1 for n arises so that the inherent buildup transient of the first-order kernel $\mathbf{h}_\mathbf{a}(k)$ will be excluded from the fitting procedure using Eq. (10). Trying to fit the transient can only degrade the procedure; confining the error minimization to the steady-state model output is the best approach.

Equations (7) and (9) can be put into a matrix formulation as follows:

$$\begin{bmatrix} a(N_1) & a(N_1-M) & \cdots & a(1) \\ a(N_1+1) & & & a(2) \\ \vdots & & & \vdots \\ a(N_t) & a(N_t-M) & \cdots & a(N_t-N_1+1) \end{bmatrix} \times \begin{bmatrix} h_a(0) \\ h_a(1) \\ \vdots \\ h_a(K_1-1) \end{bmatrix} \sim \begin{bmatrix} z(N_1) \\ z(N_1+1) \\ \vdots \\ z(N_t) \end{bmatrix}. \quad (12)$$

In matrix notation, this equation reads

$$\mathbf{Dh} \sim \mathbf{Z}, \quad (13)$$

where matrix $\mathbf{D}$ is $(N_t-N_1+1)\times K_1$, column vector $\mathbf{h}$ is $K_1 \times 1$, and column vector $\mathbf{Z}$ is $(N_t-N_1+1)\times 1$. Since data length N_t is generally a very large number, whereas the number K_1 of kernel coefficients is usually small, the attempted fit in Eqs. (12) and (13) cannot be achieved exactly. If an error sequence is defined as the difference between the left-hand and right-hand sides of Eq. (13), and the sum of squared errors is minimized, it can be shown that the optimum kernel $\mathbf{h}_0$ satisfies the equations

$$\mathbf{D'Dh}_0 = \mathbf{D'Z}, \quad \mathbf{h}_0 = (\mathbf{D'D})^{-1}\mathbf{D'Z} = (\mathbf{D'D}) \setminus (\mathbf{D'Z}). \quad (14)$$

Observe that both sides of Eq. (13) are premultiplied by $\mathbf{D}'$ and the approximation is replaced by an equals sign.

In MATLAB notation, the least-squares solution to Eq. (13) is obtained according to

$$\mathbf{h}_0 = \mathbf{D} \setminus \mathbf{Z}. \quad (15)$$

The approach in Eq. (15) instead of Eq. (14) is more advantageous, in that the condition number of square matrix $\mathbf{D'D}$ is the square of the condition number of D, which makes approach Eq. (14) less reliable.

III. CICADA EXPERIMENTS

A. Cicada field experiment with microphone

Measured data from the Tibicen chloromera and Tibicen lyricen species were recorded in the field with a parabolic microphone and a Marantz PMD670 behind a high school in West Hartford, CT. Thus, some noise from crickets and other environmental sounds contaminated the signals, but this noise was about 40–60 dB below the cicada's distinct call. Also, only distinctive, strong cicada calls—not low-level idling songs—were used to determine the existence of nonlinear behavior in the signal.

B. Cicada field experiment with laser and microphone

Another field experiment was conducted on Magicicada septendecim and Magicicada cassini in Julibee State College Park in Peoria, IL by Hughes and Katz as well as the acknowledged support. The test site was specifically chosen to amass live specimens during the 17 year emergent cycle of periodical cicadas in brood XIII. In this test, the tymbal motion of the cicada was measured by laser while the acoustic output was recorded via a microphone. This simultaneous measurement was made with dual Polytec OFV-508 optical measurement heads controlled by the Polytec electronic signal processor OFV-2802. The dual optical sensor heads allowed simultaneous measurement of the motion of both tymbals and the tymbal-to-abdomen motion. Meanwhile, the parabolic microphone was used to continuously record either the output of the two tymbals or a tymbal-abdomen experimental setup. The measurements provide the quantitative velocity from the laser, which can be transformed into displacement (position versus time) information. The tymbal motion is proportional to acoustic mechanical vibration and thus can be used in conjunction with the microphone acoustic output data. Thus, the data gathered in this field experiment, in which the output and input signals were obtained *simultaneously*, allows a unique opportunity to gain further scientific understanding of the cicada sound production system. The input signal is from the tymbal, and the output signal is recorded via the microphone. These data sets allow the application of nonlinear mathematical techniques, such as the Volterra expansion, to real-world signals.

Two channels were designated for collecting dual laser measurements of the motion of both tymbals and the tymbal-abdomen simultaneously. Most collections consisted of live wingless insects, otherwise intact. A third channel was used to record the microphone output. A fourth channel was used to time tag all signals. Two multichannel recorders were used to record and back up the data.

The experimental setup used a multichannel digital recorder set to a 96 kHz sampling rate, a laser and its controller, a backup digital recorder, and a digital timekeeper. The digital recorder facilitated the simultaneous acquisition of the tymbal motion, a microphone, and time stamp. One advantage afforded by this experimental arrangement was the opportunity to analyze quantitatively both synchronous and asynchronous tymbal motion and how such motion might impact the vocalization output.

IV. NONLINEAR SIGNAL PROCESSING RESULTS

A. Nonlinear and linear modeling of cicada signal results

A linear representation of a simulated time series of the cicada vocalization based on the superposition of a Gaussian white-noise signal passed through three parallel independent narrowband filters and the power spectral representation of this simulated time series representation is shown in Fig. 1(a). Figure 1(b) shows the temporal power spectrum of the cicada vocalization measured in the field. Given the striking similarity between these two spectra, the immediate, but erroneous, conclusion might be that the modeled spectra are a good representation of the insect's actual acoustic signature. This is the classical error made by analysts using strictly linear techniques to model behavior in a physical system. In fact, linear techniques are insufficient for a correct analysis of the underlying signal processing mechanics of the cicada's sound production system.

The simulated signal's Mi (i.e., white Gaussian excitation passed through three parallel narrowband filters) and the Gaussian Mi model of the simulated signal [from Eq. (3)] are

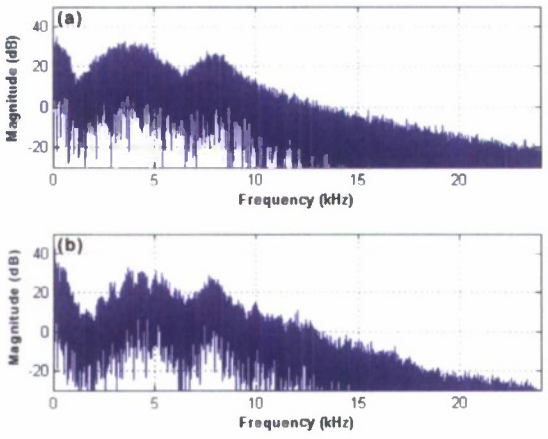

FIG. 1. (Color online) Power spectra of simulation vs field measurement. (a) Power spectrum of simulated cicada call estimated with linear model. (b) Temporal power spectrum of cicada call as measured in the field. The spectra appear similar, hut the linear model does not accurately represent the measured acoustic signature.

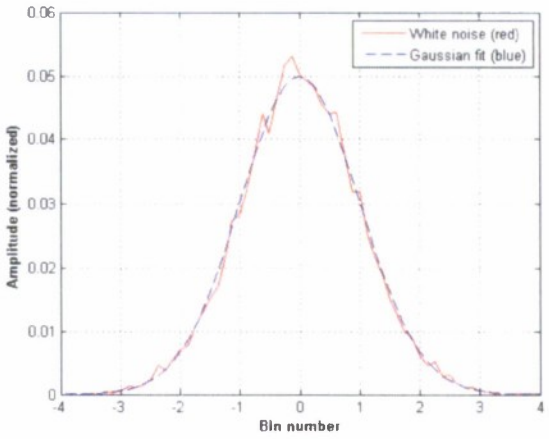

FIG. 3. (Color online) The Gaussian curve fit to the prohability density function (dashed line) is very similar to the simulated data curve hased on its histogram (solid line)—textbook example of results for a linear Gaussian process and baseline for the field measurements of cicada signals.

compared, which produce an idcntical plot to Fig. 2 where the solid line is the Mi and the "×" or cross symbol indicates the Gaussian rule. However, Fig. 2 compares a plot of the Mi obtained from the non-phase-randomized simulated date with the phase-randomized simulated data. As expected, thc phase-randomized signal and the non-phase-randomized signal Mi generate the same values since phase randomization implies near Gaussianity (according to the central limit theorem), which in turn implies linearity. In Fig. 3, the Gaussian curve fit to the probability density function (PDF) is very similar to the simulatcd data curve based on its histogram. Thcsc graphs arc like textbook examplcs of what the results should be for a linear Gaussian process. The graphs also serve as a baselinc with which to compare the field measurements of cicada signals. A field recording of the cicada signal is displayed in Fig. 4(a), with a zoomed-in version of the same signal in Fig. 4(b). The expanded view illustrates the complexity of the cicada call. In Fig. 5, the cicada data (as Mi of the cicada vocalization) are compared with the surrogate data (the phase-randomized cicada data) to show how the phase-randomized cicada signal approaches the Gaussian rule. The separation between Mi plots of the cicada signal and the phase-randomized version of the same signal corroborate its non-Gaussian probability distribution. Also, the separation between the Mi of the cicada vocalization and the simulated data using the Gaussian rule is identical to Fig. 5, which is consistent with strong non-Gaussianity [i.e., Eq. (3)].

Additional evidence of the non-Gaussian behavior of the cicada vocalization is illustrated in Fig. 6. This figure compares the Gaussian fit with the curve based on the histogram associated with the cicada's non-Gaussian signal. Note that the non-Gaussian behavior in the cicada call was not reflected in the modeled spectra shown earlier in Fig. 1. Thus, Fig. 6 reinforces the point made earlier against relying solely on power spectral techniques to analyze cicada time waveforms.

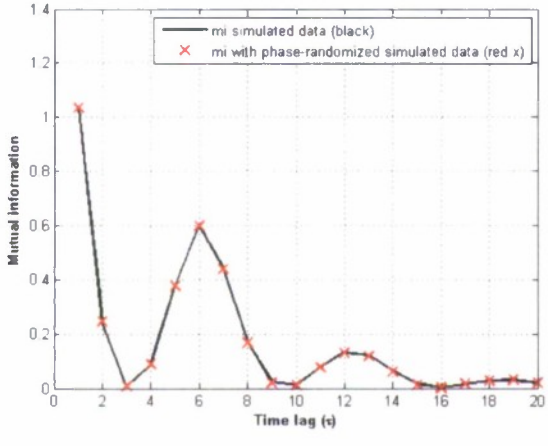

FIG. 2. (Color online) Mi obtained from the phase-randomized simulated signal as a function of the time lag τ (×) compared with the non-phase-randomized simulated data (solid line plot). The marker (×) is indistinguishable from the solid line, as expected, since phase randomization implies near Gaussianity (according to the central limit theorem), which in turn implies linearity. If plotted, the simulated signal's Mi—white Gaussian excitation passed through three narrowband filters—as a function of the time lag τ (solid line) is compared with the Gaussian rule model of the simulated signal from Eq. (3) (×). The plots are identical to what is shown.

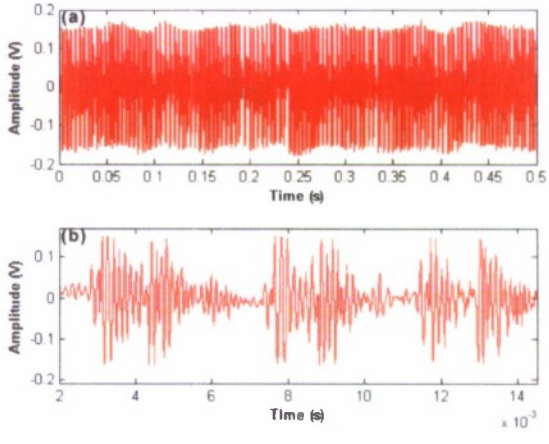

FIG. 4. (Color online) Time series of measured cicada vocalization: a 0.5 s field recording (a) and an expanded segment illustrating thc complexity of the cicada call (b).

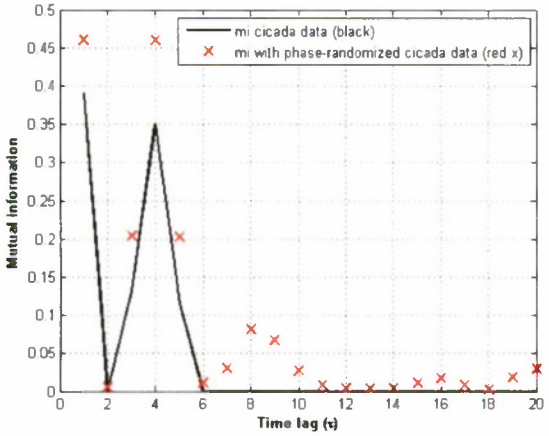

FIG. 5. (Color online) Mi of the cicada vocalization as a function of the time lag τ (solid line) compared with the surrogate data, i.e., Mi of the phase-randomized cicada data (×). The separation between Mi plots of the cicada signal and the phase-randomized version of the same signal confirm its non-Gaussian probability distribution. If plotted, the cicada signal's Mi as a function of the time lag τ (solid line) is compared with the Gaussian rule model of the signal from Eq. (3). (×) is identical to this plot.

B. Results of higher-order spectral technique using MSB

The results from Eq. (4) are shown in this section of the report. Namely, the bicoherence indicates whether the time series data is linear or nonlinear. The theoretical MSB $B(f_1,f_2)$ of a linear process is flat throughout the f_1-f_2 plane. Therefore, the example shown in Fig. 7 with an exact solution is utilized to ascertain if the bicoherence will always predict a flat surface for this linear process, where the center frequency (f_c) is zero. Here is a zero-mean, unit-variance Gaussian process. Consider the entire expression of Eq. (4) with the denominator terms containing the individual frequencies as well as the addition of both frequencies. Figure 8 illustrates that the denominator terms do not completely flatten the conical peak when the numerator (bispectrum) is divided by the denominator shown in Eq. (4). Note that the MSB plot is not flat suggesting that the process is not linear. Figure 9 illustrates that the PDF does have an effect on the random amplitudes generated in the bicoherence computation. However, the amplitudes of the sample MSB in Fig. 9 also suggest that averaging may help reduce the peaks and valleys of the plots. Figure 10 confirms that averaging does reduce the amplitude variation of the sample MSB. Such observations are consistent with the bias and variance reduction observed in coherence estimation.[33] Nonetheless, the amplitude variation is not completely removed from the estimate. Hence, averaging the MSB only scales down the problem of a fluctuating surface. Consequently, a flatness factor could yield a meaningful parameter to employ on the variations calculated for the sample MSB.

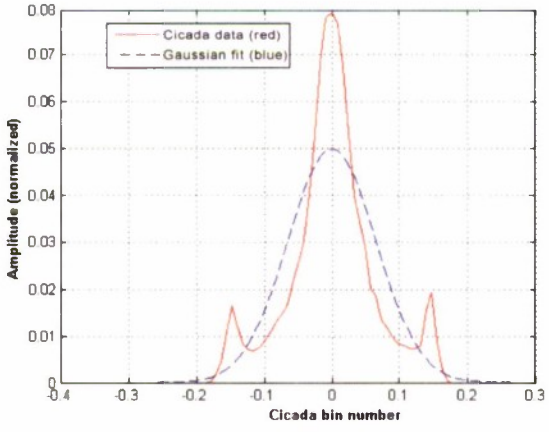

FIG. 6. (Color online) The PDF of the cicada signal (solid line, multiple peaks) compared with a Gaussian curve fit to the PDF (dashed line, single peak). The separation of the plots is additional evidence of the non-Gaussian behavior of the cicada signal.

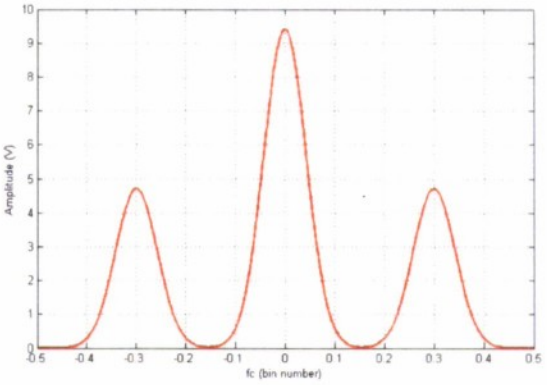

FIG. 7. (Color online) The spectrum of nonlinear function $g(t)^2-1$ provides an opportunity to assess the capability of the MSB to evaluate nonlinearity.

$$\bar{x}=\frac{1}{N}\sum_{i=1}^{N}x_i,$$

$$\sigma=\sqrt{\frac{1}{N-1}\sum_{i=1}^{N}(x_i-\bar{x})^2}, \tag{16}$$

$$\sigma_{\mathrm{MSB}}=\sqrt{\frac{1}{N-1}\sum_{i=1}^{N}(\sigma_1-\sigma_2)^2}.$$

Equation (16) defines the "flatness factor," which derives from the sample standard deviation of the fluctuations in the f_1-f_2 plane. The variable σ represents the calculation of the sample standard deviation for a known sample set $\{x_i\}$ with a total sample size N, while the parameter $\bar{x}$ is the sample

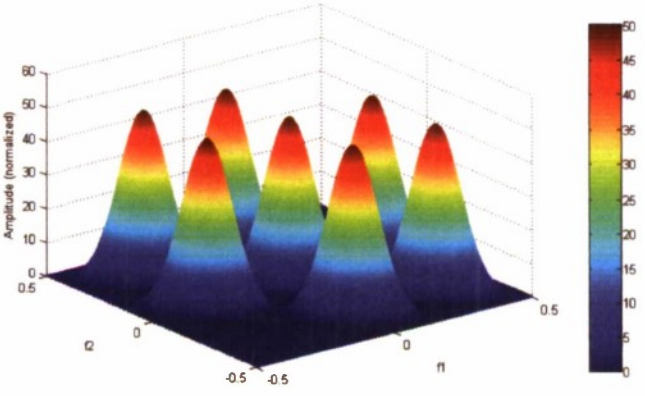

FIG. 8. The amplitude of the MSB for $g(t)^2-1$ is large despite the denominator attempting to scale the numerator (bispectrum).

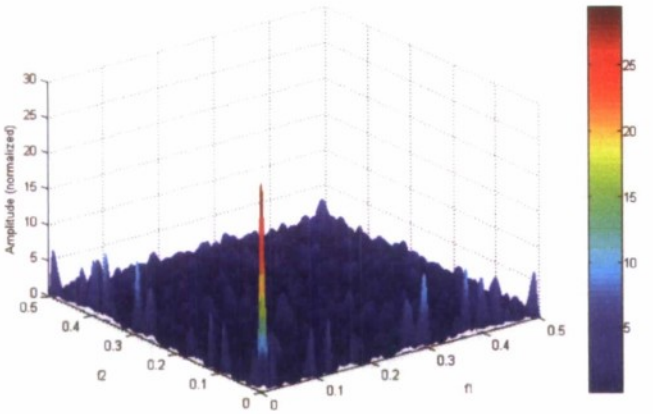

FIG. 9. The MSB is calculated for a normalized random noise signal and the mesh plot exposes that surface undulations are present in the f_1-f_2 plane, which would give the false conclusion that Gaussian random noise is not a linear process.

mean of the data set. Therefore, the sample standard deviation σ_{MSB} represents the variation for the entire plane.

Since the PDF of a given data set affects the standard derivation, a determination must be made to show how the PDF affects the MSB. A cumulative distribution function (CDF) is a convenient approach to determine if a PDF has Gaussian characteristics, which is the case for the exponential and normal distributions. If the exponential and the normal CDFs differ, the implication is that the PDF influences the MSB significantly. In Fig. 11, the CDF for the exponential signal is shown. Compared to Fig. 12, there is a difference in value of the accumulation of bins in the MSB for the exponential and normal distributions of 0.5–0.95, respectively. This difference is considerable and thus indicates that the PDF of the data contributes notably to the MSB. Consequently, a prerequisite algorithm must account for the effect of the PDF on the MSB, and PDFs could vary between individual cicadas and even more so with different species. Because the MSB significantly depends on the PDF, additional work beyond the scope of the present research is required for quantifying how statistically useful the sample MSB is for analyzing cicada signals.[35,36]

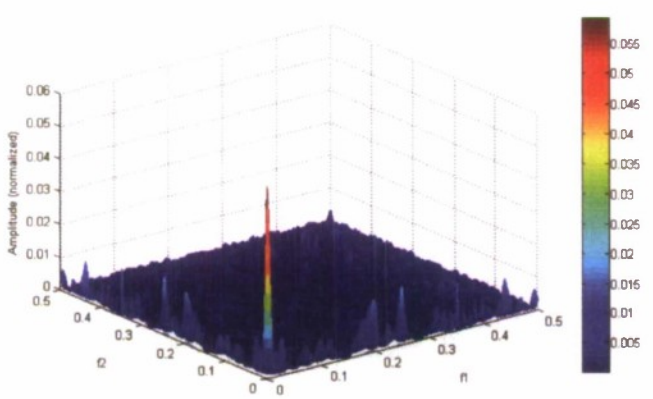

FIG. 10. The mesh plot of MSB for a normalized random noise averaged over 1000 trials still has ripples on the f_1-f_2 plane. However, this averaging scales the fluctuating surface but determining nonlinearity remains difficult to quantify.

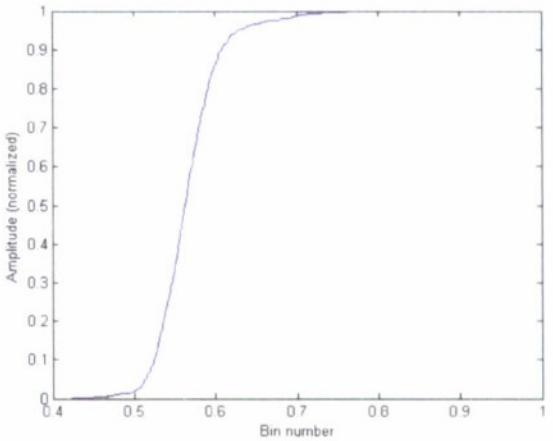

FIG. 11. (Color online) A CDF for an exponential random noise averaged over 1000 trials indicates the Gaussian characteristics of the MSB.

C. Volterra expansion method applied to cicada experimental results

A sample of 100,000 data points from the laser and microphone measurements is selected for fitting purposes, using a decimation factor $M=4$. The number of coefficients employed for the first-order fit is $K_1=100$, and the number used for the second order is $K_2=50$, which results in solving for a total of $K=5251$ coefficients. The execution time required simply to fill the $\mathbf{D}'\mathbf{D}$ matrix, using segment length $L=1000$, is 1670 s on a 2.4 GHz computer. The solution time for the optimum kernel is 22 s, and the time required to compute all five individual component waveforms $\mathbf{y_a}(n)$, $\mathbf{y_b}(n)$, $\mathbf{y_{aa}}(n)$, $\mathbf{y_{bb}}(n)$, and $\mathbf{y_{ab}}(n)$ in Eq. (9) is 220 s. The singular value decomposition of matrix $\mathbf{D}'\mathbf{D}$ took 720 s, and its condition number is 7.2×10^6. Thus, approximately 8 decimal digits (out of 15) of significance remain in the numerical results obtained. The total execution time is almost 44 min. The ratio of the power in the *total* model output, per Eq. (6), to the power in the measured microphone output $\mathbf{z}(n)$ is 0.41. Thus, the Volterra fitting procedure of the second order is capable of representing 41% of the power of the microphone waveform.

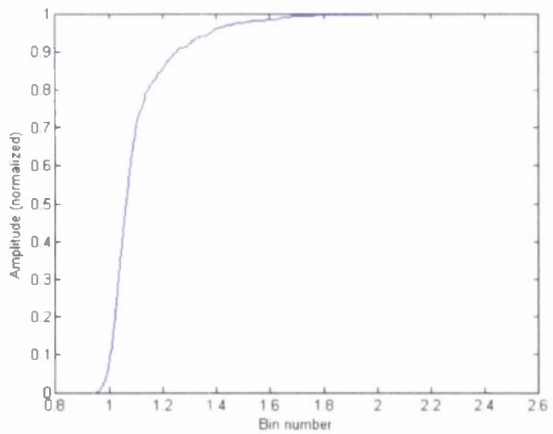

FIG. 12. (Color online) CDF for a normal random noise averaged over 1000 trials is also Gaussian but has a significant different PDF, which affects the MSB when compared to the exponential random noise in Fig. 11.

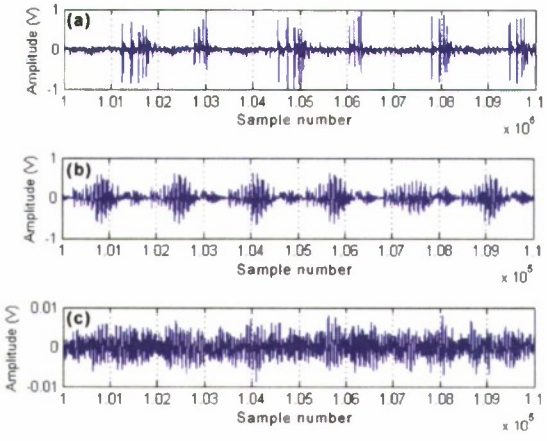

FIG. 13. (Color online) Short time segments of simultaneous laser measurements of the motion of the two tymbals and the sound output at the microphone in the field are shown. The repeated bursts of narrowband energy are clear in the laser A and B measurements in (a) and (b), respectively. The microphone output (c) tends to capture environmental noise, which blurs the individual bursts seen in (a) and (b).

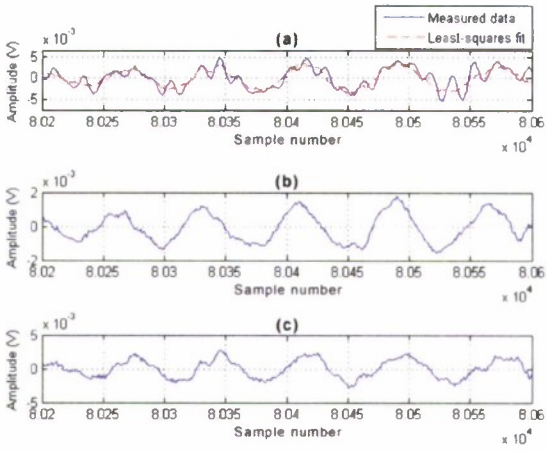

FIG. 15. (Color online) Least-squares fit for Volterra expansion. (a) A segment of the microphone data (solid line) [see Fig. 13(c)] is compared with the total fitted waveform (dashed line). The fit is rather good in some time intervals, but poorer in others—a manifestation of the fitted power ratio of 0.41. (b) and (c) are the individual total first- and second-order fits, respectively.

As a check case, an unrelated random white-noise process replaces the microphone output $\mathbf{z}(n)$, and the fitting procedure is repeated with identical parameters. The power ratio of the final fit is reduced to 0.053. An additional run with a different random sequence for $\mathbf{z}(n)$ yields a comparable value for the power ratio. Thus, the fitting ratio 0.41 that is actually attained is a significant value and indicates that nonlinearities are present in the cicada system between laser inputs and microphone output. In fact, the power in the second-order component $\mathbf{y}_2(n)$ in Eq. (9) is almost three times greater than the power in the linear component $\mathbf{y}_1(n)$. Also, the power in the cross component $\mathbf{y}_{\mathbf{ab}}(n)$ is *greater* than the powers in the two autocomponents $\mathbf{y}_{\mathbf{aa}}(n)$ and $\mathbf{y}_{\mathbf{bb}}(n)$.

D. Volterra graphical results

A short time segment of the three simultaneous field measurements is displayed in Fig 13. Each of the lasers—A and B—measured the narrowband buckling of a single cicada tymbal, shown in Figs. 13(a) and 13(b), respectively, while the microphone [see Fig. 13(c)] tended to capture all the acoustic noise in that segment of the field measurement. The corresponding (unsmoothed) spectral estimates of the complete data segments used in the Volterra fit are plotted in Fig. 14. A segment of the microphone data $\mathbf{z}(n)$ is compared with the total fitted waveform $\mathbf{y}(n)$ in Fig. 15(a). The fit is rather good in some time intervals but poorer in others—a manifestation of the actual fitted power ratio of 0.41. The plots in Figs. 15(b) and 15(c) show the individual total first-order and total second-order fits, respectively. The two first-order time-domain kernels are plotted in Fig. 16, while their complex frequency-domain transfer functions are displayed in Fig. 17. The decimation factor $M=4$ is the reason for the upper frequency limit of 12 kHz for these kernels.

An alterative Volterra expansion is computed that measures the nonlinearity in the cicada's mating call. Table I describes each tymbal's contribution to the first-and-second-order components in the cicada signal by using a Volterra expansion with $M=3$ and $K_2=70$. The Volterra technique

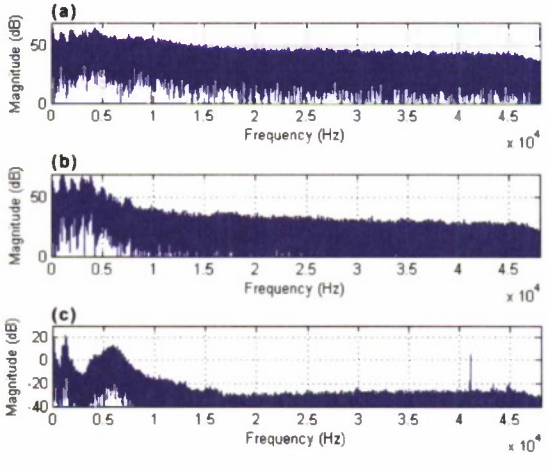

FIG. 14. (Color online) Unsmoothed spectral estimates of the data measured at lasers A (a) and B (b) and at the microphone (c). These complete data segments, corresponding to both tymbal and microphone outputs in Fig. 13, are used in the Volterra fit.

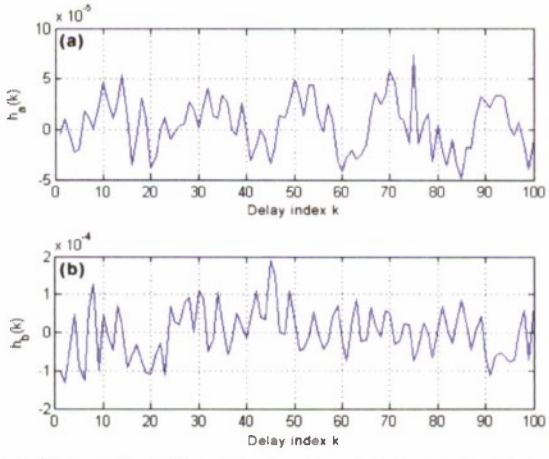

FIG. 16. (Color online) First-order time-domain kernels of tymbal motion measured by lasers A (a) and B (b).

requires both output and input functions: in this case, microphone data **zz** are the output, and the input functions are laser A and laser B. Variable **y** in Table I represents the Volterra expansion solution. The lowercase a and b for the Volterra expansion correspond to the measured vibration from the two tymbals. The first-order and second-order Volterra solutions are $\mathbf{y}_1$ and $\mathbf{y}_2$, respectively. Therefore, $\mathbf{y_a}$ is the first-order solution for laser A, $\mathbf{y_b}$ is the first-order solution for laser B, and $\mathbf{y_{aa}}$ represents the second-order solution for laser A, and so forth. The combination of both tymbals $\mathbf{y_{ab}}$ is a mixed second-order component that contributes approximately 36% of the second-order Volterra solution. This finding suggests that parametric generation may contribute to the cicada's sound propagation.[37] Also, the second-order solution contains 87% of the Volterra solution, which also indicates significant nonlinearity in the cicada call.

There are two reasons that the fitting fraction is not greater than 0.41 or 0.36 in the cases above. The common length $K_1=100$ of the two first-order kernels $\mathbf{h_a}(k)$ and $\mathbf{h_b}(k)$ is apparently adequate because both of the estimated first-order kernels decayed essentially to zero at both ends of the memory interval of length MK_1. Because the microphone data contained a considerable amount of background noise, the common length $K_2=50$ of the three second-order kernels $\mathbf{h_{aa}}(k,j)$, $\mathbf{h_{bb}}(k,j)$, and $\mathbf{h_{ab}}(k,j)$ is inadequate because the estimate does not decay sufficiently by the edges of the $k-j$ plane. The common length $K_2=70$ did reduce the decay in the kernel, but still more delay is required.

E. Implications of cicada signal results for underwater acoustics

In the commercial world, small active "fish-finding" sonars with wristband receivers are sold at a modest price to sports fishermen. Recent scientific advances in the study of small insects generating loud acoustics in air, by Bennet-Clark,[38] suggest opportunities to transfer this technology to small-sized active sonar applications. The cicada's tymbal mechanics include a tymbal plate, four ribs and resilin pad. "The four ribs of the Tymbal buckle inwards from posterior to anterior.... A train of four sound pulses [was produced], each corresponding to the inward buckling on one rib...."[38] The difference in the frequencies "suggests that the mass-to-stiffness ratio that determines the resonant frequencies of the various pulses differs from pulse to pulse.... Pulses produced later in the inward buckling sequence were less affected by the loading than earlier ones. This suggests that the effective mass determining the resonance in the later pulses is greater than that in the earlier pulses.... The Tymbal appears to act as an energy storage mechanism that releases energy as the tymbal ribs buckle inwards in sequence.... It [also] appears that the central part of each rib is decoupled from its predecessor as it buckles inwards.... observations suggest that the vibration is initially non-linear when the amplitude of vibration is largest but that it becomes more linear as the pulse decays."[38] In certain regions of interest, Bennet-Clark suggests that the resonance "is determined by the simple interaction between linear mass, compliance and damping elements."[38] Moreover, Young and Bennet-Clark suggest "that the inward movement of the tymbal plate and rib 1 will be constrained by the resilin sheet that couple it to the next, unbuckled, rib."[39] Bennet-Clark states that the "change in relative resonance frequency implies the ratio between the mass and the stiffness of the vibrating system alters as successive ribs buckle."[38] Young and Bennet-Clark go on to observe that "analogous mechanisms for producing long coherent waveforms by a succession of impulses have been modeled in bush crickets."[39] Part of the cicada's sound generation relies on the rubber-like resilin material which "acts as an energy store in which muscle work is stored comparatively slowly (perhaps during the first 2 to 4 ms of contraction) and is then released rapidly by the sudden buckling of the tymbal ribs over a period of one cycle or 230 microsec."[39] Note that 230 μs is 0.23 ms, and, thus, for 2.3 ms (between 2 and 4 ms), the discharge occurs in nominally ten times less time. This detailed description of the cidada's storage and release mechanism provides useful insight for construction of an underwater acoustic source.

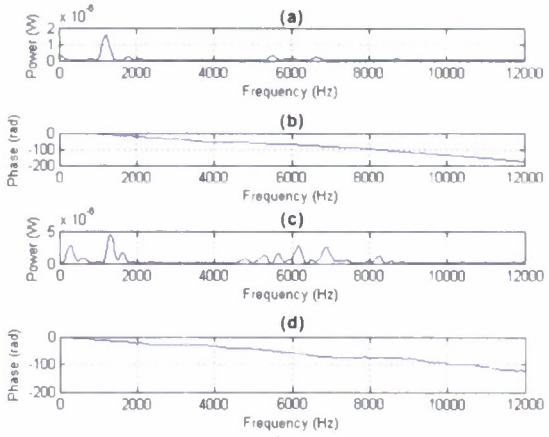

FIG. 17. (Color online) Transfer functions of first-order time-domain kernels of tymbal motion: power (a) and phase (b) for laser A data, and power (c) and phase (d) for laser B data.

V. CONCLUSIONS

This research utilizing advanced signal processing techniques to support that the cicada's loud mating call is produced as a non-Gaussian, nonlinear vocalization. Calculating the Mi to determine nonlinearity is often difficult because of the many degrees of freedom (i.e., large sample size) required to obtain a valid joint probability function [Eq. (1)]. To circumvent size limitations on the data sample, the Volterra expansion was used to discover that the second-order kernel possesses enough of the energy in the cicada signal to

TABLE I. Volterra expansion to quantify cicada signal nonlinearity for laser A (a), laser B (b), and the microphone (zz).

Ya	Yb	Yaa	ybb	yab	Y1	Y2	Y	zz	Error
6.4677×10^{-8}	3.2090×10^{-7}	2.5461×10^{-7}	1.0602×10^{-6}	6.0081×10^{-7}	3.9690×10^{-7}	1.6650×10^{-6}	1.9100×10^{-6}	4.8180×10^{-6}	2.9090×10^{-6}

indicate nonlinear behavior. Although the curse of dimensionality pertains to the Volterra expansion, the current second-order solution is satisfactory for initiating the quantification of the nonlinear parameters for modeling and simulating purposes.

Mi and surrogate hypothesis testing techniques can be combined with the Volterra or Wiener expansion to parametrize the cicada's abdominal cavity motion and tymbal excitation and create a model to simulate the insect's sound production mechanism. The combined and individual contributions of the motion of the abdomen and tymbals can be evaluated and quantified using the nonlinear least-squares technique combined with a Wiener expansion. The Wiener method allows the computation of second- and third-order solutions with fewer coefficients. Reducing the coefficient size for each order makes the computational limitation less of a concern, and consideration can be given to calculating higher-order kernels. Determining these parameters will aid in developing a device that generates sound propagation with the efficiency of the cicada vocalizations. Such efficient sound wave propagation, if viable in water, would markedly enhance source radiation efficiency for a variety of sonar applications.

ACKNOWLEDGMENTS

This study was funded by the Office of Naval Research, program manager Dr. Joel Davis. In addition, the Naval Undersea Warfare Center Division, Newport, RI provided the lasers and the initial signal processing analysis for the laser data. The authors are specifically grateful to Dr. Paul Lefebvre, Dr. Pierre Corriveau, and Mr. Joseph Monti for their support of the experiment. The authors are also grateful to Dr. John Cooley for providing his knowledge of several species of cicada as well as his expertise in producing mating calls, to Mr. Michael Neckermann and Mr. Gerry Bunker for helping in the laser field experiment, and to Dr. Lynn Antonelli for her technical consultations on effectively using the dual-headed laser to record this historic data.

[1]H. C. Bennet-Clark, "Tymbal mechanics and the control of song frequency in the cicada Cyclochila australasiae," J. Exp. Biol. **200**, 1681–1694 (1997).

[2]H. C. Bennet-Clark, "Size and scale effects as constraints in insect sound communication," Philos. Trans. R. Soc. London, Ser. B **353**, 407–419 (1998).

[3]H. C. Bennet-Clark, "Resonators in insect sound production: How insects produce loud pure-tone songs," J. Exp. Biol. **202**, 3347–3357 (1999).

[4]H. C. Bennet-Clark and A. G. Daws, "Transduction of mechanical energy into sound energy in the cicada Cyclochila australasiae," J. Exp. Biol. **202**, 1803–1817 (1999).

[5]H. C. Bennet-Clark and D. Young, "The scaling of song frequency in cicadas," J. Exp. Biol. **191**, 291–294 (1994).

[6]H. C. Bennet-Clark and D. Young, "Sound radiation by the bladder cicada Cystosoma saundersii," J. Exp. Biol. **201**, 701–715 (1998).

[7]R. MacNally and D. Young, "Song energetics of the bladder cicada, Cystosoma saundersii," J. Exp. Biol. **90**, 185–196 (1980).

[8]J. R. Cooley and D. C. Marshall, "Sexual signaling in periodical cicadas, Magicicada spp. (Hemiptera: Cicadidae)," Behaviour **138**, 827–855 (2001).

[9]J. S. Dugdale and C. A. Fleming, "Two New Zealand cicadas collected on Cook's Endeavour Voyage, with description of a new genus," New Zealand J. Sci. **12**, 929–957 (1969).

[10]D. H. Lane, "The recognition concept of species applied in an analysis of putative hybridization in New Zealand cicadas of the genus Kikihia (Insecta: Hemiptera: Tibicinidae)," in *Speciation and the Recognition Concept: Theory and Application*, edited by D. M. Lambert and H. G. Spencer (Johns Hopkins University Press, Baltimore, 1995), pp. 367–421.

[11]C. L. Marlatt, "The periodical cicada," U.S. Dept. Agric. Bur. Entomol. Bull. **71**, 1–181 (1907).

[12]R. D. Alexander and T. E. Moore, "The evolutionary relationships of 17-year and 13-year cicadas, and three new species (Homoptera, Cicadidae, Magicicada)," U. Mich. Zoo. Misc. Pub. **121**, 1–59 (1962).

[13]D. Young and R. Josephson, "Pure-tone songs in cicadas with special reference to the genus Magicicada," J. Comp. Physiol. **152**, 197–207 (1983).

[14]H. C. Bennet-Clark and D. Young, "A model of the mechanism of sound production in cicadas," J. Exp. Biol. **173**, 123–153 (1992).

[15]P. J. Fonseca and A. V. Popov, "Sound radiation in a cicada: The role of different structures," J. Comp. Physiol., A **175**, 349–361 (1994).

[16]D. Young and H. C. Bennet-Clark, "The role of the tymbals in cicada sound production," J. Exp. Biol. **198**, 1001–1019 (1995).

[17]P. J. Fonseca and R. M. Hennig, "Phasic action of the tensor muscle modulates the calling song in cicadas," J. Exp. Biol. **199**, 1535–1544 (1996).

[18]P. J. Fonseca and A. V. Popov, "Directionality of the tympanal vibrations in a cicada: A biophysical analysis," J. Comp. Physiol., A **180**, 417–427 (1997).

[19]P. J. Fonseca and H. C. Bennet-Clark, "Asymmetry of tymbal action and structure in a cicada: A possible role in the production of complex songs," J. Exp. Biol. **201**, 717–730 (1998).

[20]N. H. Fletcher, *Acoustic Systems in Biology* (Oxford University Press, New York, 1992).

[21]G. W. Pierce, *The Songs of Insects* (Harvard University Press, Cambridge, 1948).

[22]W. J. Bailey, *Acoustic Behavior of Insects: An Evolutionary Perspective* (Chapman and Hall, New York, 1991).

[23]V. B. Wigglesworth, *The Principles of Insect Physiology* (Chapman and Hall, London, 1972).

[24]H. C. Gerhardt and F. Huber, *Acoustic Communication in Insects and Anurans: Common Problems and Diverse Solutions* (University of Chicago Press, Chicago, 2002).

[25]A. W. Ewing, *Arthropod Bioacoustics: Neurobiology and Behaviour* (Comstock, Ithaca, NY, 1989).

[26]J. E. Treherne, *Insect Neurobiology* (Elsevier, New York, 1974).

[27]B. Lewis, *Bioacoustics: A Comparative Approach* (Academic, New York, 1983).

[28]M. D. Atkins, *Introduction to Insect Behavior* (Macmillan, New York, 1980).

[29]S. P. Timoshenko and J. M. Gere, *Mechanics of Materials*, 3rd ed. (PWS, Boston, MA, 1990).

[30]H. D. I. Abarbanel, *Analysis of Observed Chaotic Data* (Springer-Verlag, New York, 1996) p. 28.

[31]J. Theiler, S. Eubank, A. Longtin, B. Galdrikian, and J. D. Farmer, "Testing for nonlinearity in time series: The method of surrogate data," IUTAM Symposium and NATO Advanced Research Workshop on Interpretation of Time Series for Nonlinear Mechanical Systems, University of Warwick, Coventry, UK, August 1991.

[32]F. M. Reza, *An Introduction to Information Theory* (Dover, New York, 1994) p. 283.

[33]G. C. Carter, *Coherence and Time Delay Estimation: An Applied Tutorial for Research, Development, Test, and Evaluation Engineers* (IEEE, Piscataway, NJ, 1993).

[34]M. Schetzen, *The Volterra and Wiener Theories of Nonlinear Systems*, revised ed. (Krieger, Malabar, FL, 2006).

[35]M. J. Hinich, E. M. Mendes, and L. Stone "Detecting Nonlinearity in Time Series: Surrogate and Bootstrap Approaches," *Studies in Nonlinear Dynamics & Econometrics* (The Berkeley Electronic Press, Berkeley, CA, 2005), Vol. **9**, No. 4, Art. 3.

[36]D. M. Patterson and R. A. Ashley, *A Nonlinear Time Series Workshop: A Toolkit for Detecting and Identifying Nonlinear Serial Dependence* (Kluwer Academic, Boston, MA, 2000).

[37]M. B. Moffett and R. H. Mellen, "Model for Parametric Acoustic Sources," J. Acoust. Soc. Am. **61**, 325–337 (1977).

[38]H. C. Bennet-Clark, "Tymbal mechanics and the control of song frequency in the cicada Cyclochila australasiae," J. Exp. Biol. **200**, 1681–1694 (1997).

[39]D. Young and H. C. Bennet-Clark, "The role of the tymbal in cicada sound production," J. Exp. Biol. **198**, 1001–1019 (1995).

INITIAL DISTRIBUTION LIST

Addressee	No. of Copies
Defense Advanced Research Projects Agency (Deborah Furey)	2
Office of Naval Research (Frank Herr)	2
Naval Postgraduate School (RADM R. Jones, Kevin Smith, Daphne Kapolka (2))	4
Defense Technical Information Center	2